АСТРОФИЗИКА

ТОМ 67 АВГУСТ, 2024 ВЫПУСК 3

DOI: 10.54503/0571-7132-2024.67.3-325

REANALYZING THE LIGHT CURVES AND ABSOLUTE PARAMETERS OF TWENTY CONTACT BINARY STARS USING TESS DATA

E.PAKI, A.PORO

Received 28 May 2024
Accepted 26 August 2024

Reanalyzing contact binaries with space-based photometric data and investigating possible parameter changes can yield accurate samples for theoretical studies. We investigated light curve solutions and fundamental parameters for twenty contact binary systems. The most recent Transiting Exoplanet Survey Satellite (TESS) data is used to analyze. The target systems in the investigation have an orbital period of less than 0.58 days. Light curve solutions were performed using the PHysics Of Eclipsing BinariEs (PHOEBE) Python code version 2.4.9. The results show that systems had various mass ratios from $q = 0.149$ to $q = 3.915$, fillout factors (the degree of contact) from $f = 0.072$ to $f = 0.566$, and inclinations from $i = 52^{o}.8$ to $i = 87^{o}.3$. The effective temperature of the stars was less than 7016 K, which was expected given the features of most contact binary stars. Twelve of the target systems' light curves were asymmetrical in the maxima, showing the O'Connell effect, and a starspot was required for light curve solutions. The estimation of the absolute parameters of the binary systems was presented using the $a - P$ empirical relationship and discussed. The orbital angular momentum J_0 of the systems was calculated. The positions of the systems were also depicted on the $M - L$, $M - R$, $q - L_{ratio}$, $M_{tot} - J_0$, and $T - M$ diagrams.

Keywords: *binaries: eclipsing - binaries: close - data analysis*

1. *Introduction*. Eclipsing binaries are important in investigating stellar formation and structure, examining stellar evolution theories, and determining stars' physical properties. Binary systems were first classified into three types based on the light curves' shapes: Algol (EA), β Lyrae (EB), and W Ursae Majoris (W UMa, EW). Then, a more precise classification was provided by Kopal [1], which was based on Roche geometry, binary systems were classified as detached, semi-detached, and contact. Contact binary systems are one of the most interesting kinds of stellar binaries among observers and researchers. Contact systems' stars have filled their Roche lobes [1], and the temperature difference between these stars is close to each other [2]. Some of them are known as low-mass and Low-Temperature Contact Binaries (LTCBs) systems [3].

According to the Binnendijk [4] study, contact binaries can be divided into A and W subtypes. The more massive component has a higher effective temperature in the A-subtype, and if the less massive component has a higher effective

temperature, it is classified as a W-subtype. These subtypes are still being discussed, and for a better understanding, it is necessary to determine and analyze a large number of contact systems in terms of fundamental parameters.

The stars of contact systems are transferring mass to each other [5], and in this process, their orbital periods can be changed. The orbital period of contact systems plays a role in relations with absolute parameters, and they are effective in the evolutionary process of these systems [6,7]. There have been several studies conducted on the upper and lower cut-offs of these systems' orbital periods [8]. The investigations show that contact systems' orbital periods usually lie between 0.2 and 0.6 days.

One of the prominent features in many contact systems is the presence of starspot(s) induced by the stars' magnetic activities. Hot or cold starspots, which are required for the light curve solution, are explained by the O'Connell effect [9]. The effect of starspots can be seen on the asymmetric maxima of the light curve.

There are unsolved issues related to contact binary systems, parameter relationships, and the evolution of stars [10]. This requires precisely defined elements from further contact binary samples [11]. Even in the case of well-studied systems, it will be important to carry out investigations due to issues with phasing, challenging novel discoveries, and evolutionary status.

In the following sections, we present the general specifications of target systems in catalogs and literature (Section 2), light curve solutions of 20 contact binary systems (Section 3), estimating absolute parameters (Section 4), and finally a discussion and conclusion (Section 5).

2. *Tartget systems and dataset.*

2.1. *Systems' selection.* We considered twenty contact binary systems for light curve analysis and estimation of absolute parameters. The selected studies for these target systems have considered the mass ratio based on spectroscopic results. We used these mass ratios as the initials for the light curve analysis. Due to the passage of time compared to some selected studies and spectroscopic quality, the final mass ratios may change slightly in this study.

Except for DY Cet [12], which has performed light curve analysis using TESS Sector 4 data, other systems have been studied previously using just ground-based data. Some parameters can be obtained from spectroscopic data analysis; however, most of the light curve elements are determined from photometric data. Therefore, the accuracy of photometric data has a significant impact on the results of the light curve solutions and then on the estimation of absolute parameters. Therefore, by using suitable quality TESS data, parameters may be obtained with more appropriate accuracy.

An introduction to the target systems is available in the online version of this study: https://doi.org/10.48550/arXiv.2405.18618.

2.2. *TESS observations*. TESS provides high accuracy and high time resolution light curves of contact binary stars that promote scientific studies. The main goal of the TESS mission is to detect and classify exoplanets, and each observation sector takes about 28 days. We used TESS data for light curve analysis in this study [13-14]. TESS data are available at the Mikulski Archive for Space Telescopes (MAST). If each of the systems had several sectors in TESS, we selected the most recent available sector with good-quality data for the light curve analysis. The sector used for each system is listed in Table 1, and all of them were observed at a 120-second exposure time.

2.3. *General features*. The selected contact binary systems have orbital periods ranging from 0.22 to 0.58 days, their apparent magnitude is $8^m.14$ to $11^m.26$, and the effective temperature of star 1 (T_1) is 4300 to 6980 K in the reference studies.

Table 1 contains the names of the selected systems along with their general characteristics. Therefore, in Table 1, the RA and DEC of the systems from the SIMBAD database, the distance obtained from the Gaia DR3 parallax, the apparent magnitude of the system from the All Sky Automated Survey (ASAS) catalog, the time of minima (BJD_{TDB}) and the orbital period from the Variable Star indeX (VSX) database, and the last column, the used TESS sector, were given. We used Schlafly, Finkbeiner [15] study, and the DUST-MAPS Python package developed by Green et al. [16] to determine the extinction coefficient A_V along with its uncertainty.

3. *Light curve analysis*. The PHOEBE Python code version 2.4.9 [17] and TESS filter were used to perform light curve analysis on 20 binary systems. Based on the appearance of the light curve, the short orbital period, and the results of previous studies, we selected contact mode for the systems' light curve solutions.

Assumed values for the bolometric albedo and gravity-darkening coefficients were $A_1 = A_2 = 0.5$ (Ruciński [18]) and $g_1 = g_2 = 0.32$ (Lucy [19]). We used the Castelli, Kurucz [20] method to model the stellar atmosphere, and the limb darkening coefficients were from the PHOEBE tables. The reflection effect in contact binary systems refers to the component's irradiation of each other. We considered this effect in the light curve analysis.

We set initial effective temperatures for stars and mass ratio from reference studies and analyzed the light curves of 20 target systems (Table 2). Parameter input values were taken from studies including spectroscopic data for these target systems. The optimization tool in PHOEBE was then utilized to improve the output of light curve solutions and obtain the final results. The five main

Table 1

COORDINATES AND OTHER CHARACTERISTICS OF TARGET BINARY SYSTEMS

System	RA J2000	DEC J2000	d pc	V mag	A_V	t_0 BJD_{TDB}	P day	TESS Sector
AC Boo	14 56 28.3364	+46 21 44.0691	155.42(36)	10.27(21)	0.029(1)	2452499.9507	0.35245	50
AQ Psc	01 21 03.5557	+07 36 21.6178	133.27(37)	8.55(18)	0.079(1)	2453653.7169	0.47560	43
BI CVn	13 03 16.4093	+36 37 00.6406	221.26(2.11)	10.41(22)	0.031(1)	2444365.2503	0.38416	49
BX Dra	16 06 17.3670	+62 45 46.0898	520.27(4.65)	10.68(22)	0.048(1)	2449810.5906	0.57902	58
BX Peg	21 38 49.3911	+26 41 34.2134	149.34(56)	10.88(23)	0.076(1)	2455873.3966	0.28042	55
CC Com	12 12 06.0379	+22 31 58.6828	71.38(11)	11.21(23)	0.035(1)	2453012.8637	0.22069	49
DY Cet	02 38 33.1803	-14 17 56.7219	186.88(49)	9.47(20)	0.046(1)	2453644.7385	0.44079	4
EF Boo	14 32 30.5386	+50 49 40.6868	160.93(34)	9.63(20)	0.021(1)	2452500.2238	0.42052	50
EX Leo	10 45 06.7720	+16 20 15.6771	97.10(24)	8.91(19)	0.037(1)	2448500.0087	0.40860	46
FU Dra	15 34 45.2133	+62 16 44.3332	159.56(50)	10.68(22)	0.030(1)	2448500.2637	0.30672	51
HV Aqr	21 21 24.8100	-03 09 36.8855	154.24(2.32)	9.85(21)	0.090(1)	2452500.2191	0.37446	55
LO And	23 27 06.6850	+45 33 22.0263	290.62(3.82)	11.26(23)	0.213(2)	2456226.6800	0.38044	57
OU Ser	15 22 43.4748	+16 15 40.7337	53.29(7)	8.14(17)	0.024(1)	2448500.2787	0.29677	51
RW Com	12 33 00.2840	+26 42 58.3618	107.60(25)	11.05(23)	0.026(1)	2454918.7048	0.23735	49
RW Dor	05 18 32.5451	-68 13 32.7780	123.57(17)	11.00(23)	0.087(1)	2453466.5302	0.28546	67
RZ Com	12 35 05.0595	+23 20 14.0278	208.26(1.70)	10.34(22)	0.032(1)	2458253.6304	0.33851	49
TW Cet	01 48 54.1435	-20 53 34.5917	152.71(46)	10.40(22)	0.022(1)	2454476.6173	0.31685	3
UV Lyn	09 03 24.1259	+38 05 54.5972	143.65(36)	9.60(20)	0.036(1)	2453407.3606	0.41498	21
UX Eri	03 09 52.7437	-06 53 33.5110	237.40(1.00)	11.15(23)	0.142(1)	2454828.6698	0.44529	4
VW Boo	14 17 26.0325	+12 34 03.4469	150.05(38)	10.49(22)	0.037(1)	2452840.6121	0.34232	50

parameters (T_1, T_2, q, f, l_1) were then processed for the optimization.

The well-known O'Connell effect [9] appears by the asymmetry in the brightness of maxima in the light curve of eclipsing binary stars. The most probable reason for this phenomenon is the existence of starspot(s) caused by the components' magnetic activity [21]. Eight systems had symmetrical light curves and 12 systems needed a cold starspot for light curve analysis.

The parameters i, q, f, $T_{1,2}$, Ω, l_1/l_{tot}, and $r_{(mean)1,2}$ are estimated by modeling the TESS light curves. Table 3 presents the light curve analysis results. Fig.1 shows TESS data and synthetic light curves of the binary systems. The geometric structure of the systems in phases 0.25 or 0.75 is shown in Fig.2. The color in Fig.2 indicates the differences in temperature on the star's surface.

4. *Estimation of the absolute parameters*. There are various methods to derive absolute parameters, particularly when photometric data is utilized. In some investigations, empirical relationships or the Gaia DR3 parallax method are used to estimate absolute parameters [37,6,38]. Using Gaia DR3 parallax to

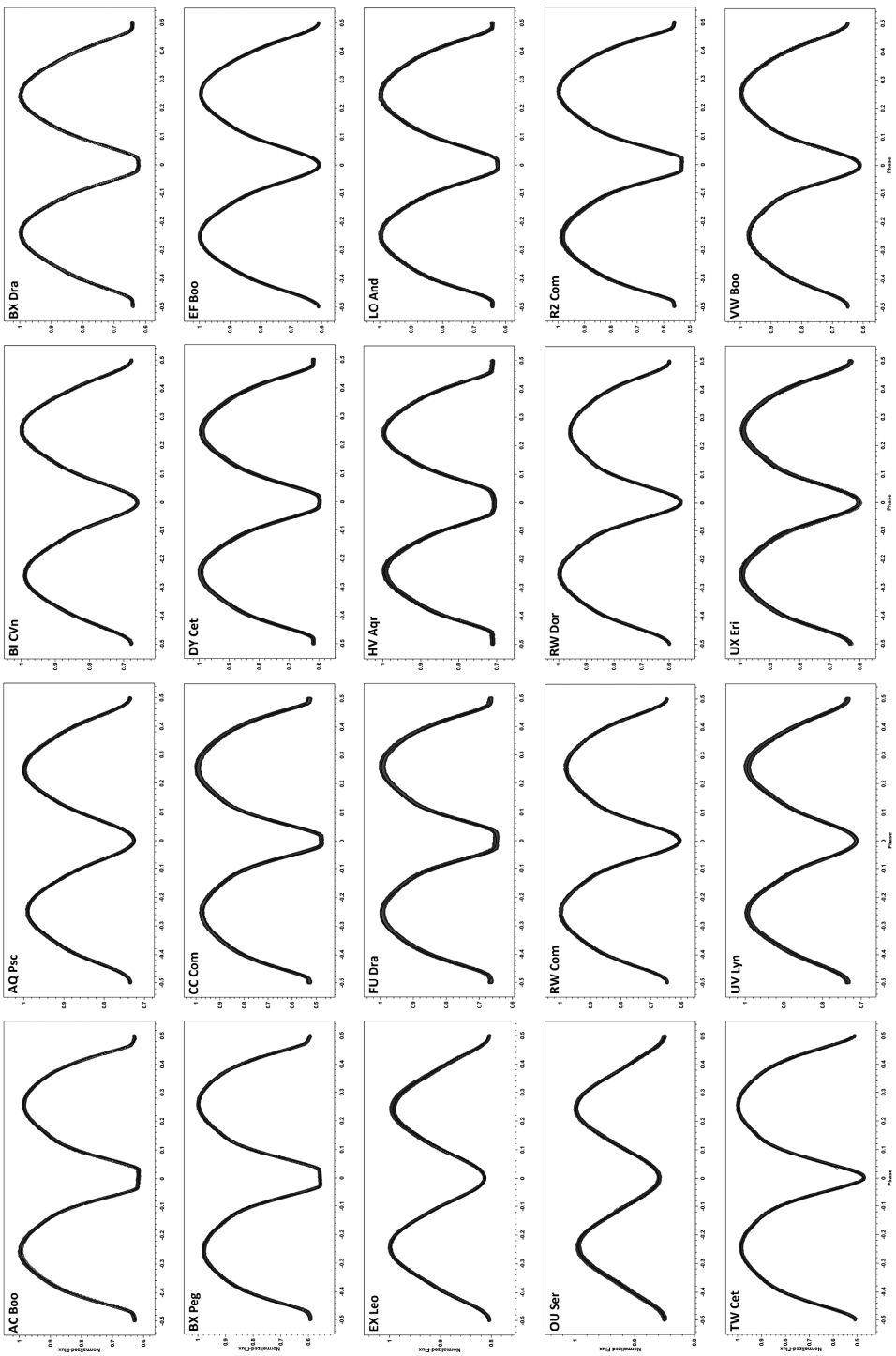

Fig.1. TESS data and synthetic light curves for the target binary systems.

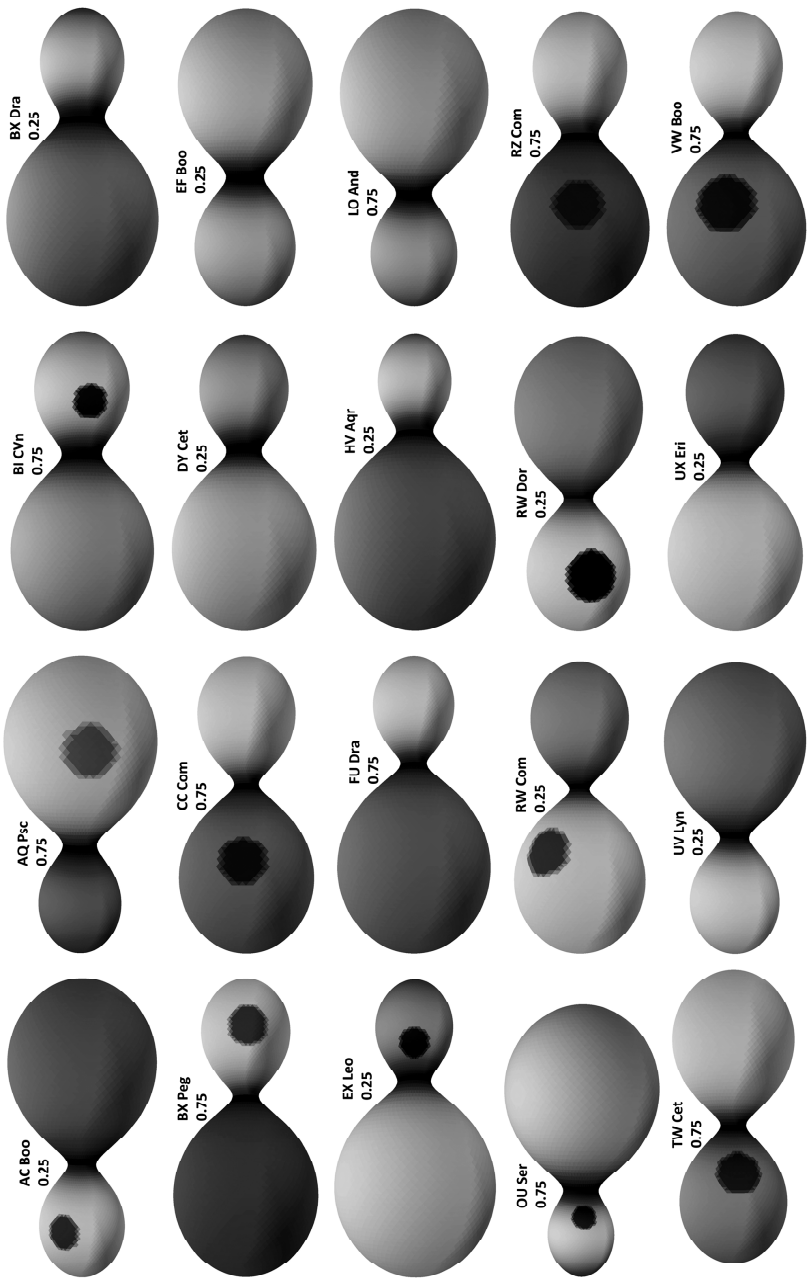

Fig.2. Three-dimensional view of the systems in phases 0.25 or 0.75.

estimate absolute parameters can have good accuracy, but there are challenges to obtaining proper accuracy. Challenges make this method unsuitable for some

binary systems investigations. For example, the parameter that is obtained from the observational data and plays an important role in the calculation process is the maximum apparent magnitude V_{max}. In the first step of the calculation process using Gaia DR3 parallax, V_{max} is used to estimate the absolute magnitude M_V. Therefore, this may not be an appropriate method for calculating the absolute parameters in ground-based observations if the light curve's maxima display more dispersion. On the other hand, the extinction coefficient A_V should also be reasonable and low value (Table 1). In some cases, the large error for the Gaia DR3 parallax is associated with a large A_V value, although either alone can overshadow the accuracy of the absolute parameter estimates. Large parallax errors usually come in systems with galactic coordinates b between +5 and -5, making it challenging to determine A_V with good accuracy [39]. Also, the initial temperature chosen for the analysis can completely affect the accuracy of the results. The study published by the Poro et al. [40] study discusses the limitations of this method. In this study, due to the lack of a reliable value of V_{max} for all target systems, we preferred not to use this method.

The mass ratio is one of the most crucial factors in the estimation of the absolute parameters. There are several methods to test or obtain mass ratios from

Table 2

LIGHT CURVE SOLUTIONS' RESULTS IN REFERENCE STUDIES OF THE SYSTEMS

System	i °	$q = M_2/M_1$	f	T_1 (K)	T_2 (K)	$\Omega_1 = \Omega_2$	Reference
AC Boo	86.3(5)	3.340(4)	0.046	6250	6241(6)	7.034(4)	[22]
AQ Psc	69.06(80)	0.266(2)	0.35	6250(157)	6024(150)	2.253(12)	[23]
BI CVn	71.30(10)	2.437(4)	0.146(11)	6125(2)	6093	5.698(4)	[24]
BX Dra	80.63(6)	0.2884(5)	0.515	6980	6979(2)	2.3475(16)	[25]
BX Peg	87.2(6)	2.66	0.171(12)	5887(7)	5300	6.057(8)	[26]
CC Com	89.8(6)	1.90(1)	0.17	4300	4200(60)	5.009	[27]
DY Cet	82.48(34)	0.356(9)	0.24	6650(178)	6611(176)	2.529(5)	[23]
EF Boo	75.7(2)	1.871	0.18	6450	6425(14)	4.921(12)	[28]
EX Leo	60.8(2)	0.2	0.35	6340	6110(14)	2.186(12)	[29]
FU Dra	80.4(2)	3.989	0.190(12)	6100	5842(6)	7.778	[30]
HV Aqr	79.186(183)	0.145	0.569(10)	6460	6669(7)	2.036	[31]
LO And	80.1(6)	0.305(4)	0.4	6650	6690(24)	2.401(9)	[32]
OU Ser	50.47(2.24)	0.173(17)	0.68	5940(144)	5759(283)	2.090(17)	[23]
RW Com	72.43(29)	0.471(6)	0.15	4830(115)	4517(98)	5.319(9)	[23]
RW Dor	77.2(1)	1.587	0.115(67)	5560	5287(10)	4.64(4)	[33]
RZ Com	86.8(6)	2.179(9)	0.11(1)	6276(200)	6070	5.393(10)	[34]
TW Cet	81.18(10)	0.75(3)	0.06	5865(152)	5753(147)	3.308(2)	[23]
UV Lyn	67.6(1)	2.685	0.18	6000	5770(5)	6.080(1)	[35]
UX Eri	75.70(23)	0.373(21)	0.18	6093(153)	6006(150)	6.065(8)	[23]
VW Boo	73.81(5)	2.336	0.108(5)	5560	5198(3)	5.626(3)	[36]

Table 3

THE RESULTS OF THE LIGHT CURVE ANALYSIS OF THE SYSTEMS IN THIS STUDY

System	i °	$q = M_2/M_1$	f	T_1 (K)	T_2 (K)	$\Omega_1 = \Omega_2$	l_1/l_{tot}	$r_{(mean)1}$	$r_{(mean)2}$	Spot
AC Boo	84.05(50)	3.364(22)	0.199(10)	6378(77)	6091(75)	6.970(34)	0.289(17)	0.292(1)	0.500(1)	1
AQ Psc	68.60(65)	0.255(27)	0.314(24)	6299(58)	5969(51)	2.314(60)	0.794(9)	0.519(2)	0.287(2)	1
BI CVn	69.36(36)	2.437(137)	0.356(12)	6186(48)	6010(46)	5.643(193)	0.345(22)	0.332(6)	0.483(5)	1
BX Dra	79.85(27)	0.259(4)	0.566(20)	6944(46)	7016(44)	2.281(11)	0.744(11)	0.531(1)	0.304(1)	0
BX Peg	87.30(39)	2.861(20)	0.154(6)	5822(73)	5357(63)	6.337(30)	0.354(21)	0.303(1)	0.484(1)	1
CC Com	85.83(56)	1.991(46)	0.113(11)	4369(60)	4154(47)	5.172(71)	0.422(7)	0.330(2)	0.450(2)	1
DY Cet	81.05(65)	0.345(8)	0.287(13)	6666(52)	6569(45)	2.503(17)	0.721(14)	0.493(2)	0.311(2)	0
EF Boo	74.77(23)	1.882(35)	0.261(9)	6412(48)	6452(48)	4.929(54)	0.363(15)	0.347(2)	0.456(2)	0
EX Leo	59.22(41)	0.172(26)	0.467(108)	6200(72)	6245(68)	2.110(71)	0.808(35)	0.556(11)	0.262(12)	1
FU Dra	78.74(29)	3.915(30)	0.164(7)	6090(46)	5848(43)	7.700(43)	0.261(11)	0.278(1)	0.511(1)	0
HV Aqr	79.35(45)	0.168(2)	0.516(21)	6495(46)	6649(53)	2.095(6)	0.802(10)	0.560(1)	0.263(1)	0
LO And	79.24(51)	0.304(8)	0.315(13)	6716(53)	6622(62)	2.415(17)	0.741(15)	0.505(2)	0.301(3)	0
OU Ser	52.82(51)	0.149(37)	0.565(192)	5852(61)	5836(67)	2.046(105)	0.829(46)	0.570(18)	0.257(21)	1
RW Com	74.14(59)	0.540(80)	0.072(11)	4779(57)	4586(49)	2.929(153)	0.669(51)	0.441(14)	0.333(13)	1
RW Dor	76.08(30)	1.590(99)	0.144(12)	5506(48)	5318(51)	4.576(152)	0.426(3)	0.352(6)	0.433(6)	1
RZ Com	85.66(16)	2.348(21)	0.293(8)	6359(60)	6004(54)	5.559(33)	0.373(16)	0.330(1)	0.476(1)	1
TW Cet	83.62(36)	0.762(56)	0.103(9)	5899(51)	5708(52)	3.307(97)	0.589(3)	0.413(6)	0.366(6)	1
UV Lyn	65.77(12)	2.696(62)	0.187(7)	5993(34)	5792(38)	6.096(87)	0.323(14)	0.310(2)	0.481(2)	0
UX Eri	75.62(42)	0.508(50)	0.146(13)	6214(69)	5878(66)	2.847(97)	0.685(35)	0.452(9)	0.333(9)	0
VW Boo	73.38(13)	2.377(85)	0.127(10)	5504(54)	5267(50)	5.700(123)	0.360(23)	0.316(3)	0.466(3)	1

photometric data [41,42]. In this study, the initial mass ratio of target systems was obtained using different qualities of spectroscopic data from reference studies. The analysis of light curves showed that the mass ratio did not change significantly compared to the reference studies.

We used the semi-major axis and orbital period (a - P) relationship for estimating absolute parameters from the study Poro et al. [39] (Eq. (1)). Considering that the uncertainties reported in Eq. (1) have upper and lower limits, we used their average for calculations.

$$a = \left(0.372^{+0.113}_{-0.114}\right) + \left(5.914^{+0.272}_{-0.298}\right) P. \quad (1)$$

Then, using the well-known equation of Kepler's third law (Eq. (2)), we obtained the total mass ($M_1 + M_2$) of the components. Since $q = M_2/M_1$, the values of each star's mass were estimated.

$$\frac{a^3}{G(M_1 + M_2)} = \frac{P^2}{4\pi^2}. \quad (2)$$

The values of r_{mean} obtained from light curve solutions (Table 3) and the radius R of each star were calculated (Eq. (3)).

$$a = \frac{R}{r}. \tag{3}$$

According to the effective temperature obtained from the light curve analysis and the calculated radius, the luminosity L was calculated (Eq. (4)).

$$L = 4\pi R^2 \sigma T^4. \tag{4}$$

The absolute bolometric magnitude of stars was calculated and $M_{bol\odot}$ considered 4.73 from the Torres [43] throughout this estimating process (Eq. (5)).

$$M_{bol} - M_{bol\odot} = -2.5 \log \frac{L}{L_\odot}. \tag{5}$$

The surface gravity of each star was also calculated based on its mass and radius (Eq. (6)).

$$g = G_\odot \frac{M}{R^2}. \tag{6}$$

The uncertainties of the absolute parameters were calculated using the errors determined by the PHOEBE code for the light curve elements used in the process, such as $T_{1,2}$, $r_{mean1,2}$, and q. Table 4 contains the results of the estimated absolute parameters.

5. *Discussion and conclusion*. We selected 20 contact binary systems and one of the latest published studies for each of them. The target systems have or used spectroscopic results. Except for DY Cet, none of them have used TESS data for analysis. Quality photometric data, like space-based data, is important for obtaining accurate light curve parameters and then estimating absolute parameters.

We conducted the light curve analysis using the PHOEBE Python code and TESS observations. We considered the effective temperature and mass ratio reported in the studies as input values. The results of the light curve analysis showed that the mass ratio of the systems has changed slightly. The minimum difference between the mass ratio of our results and reference studies is related to the BI CVn system with 0%, and the maximum difference is for the BX Peg system with 7%. The elapsed times from the reference studies and precise TESS data rather than ground-based observations can account for some of the discrepancies in the light curve analysis results.

The stars in contact binary systems have a small temperature difference due to mass and energy transfer [6]. The difference in effective temperature between the two stars in the BX Peg system had the maximum value at 465 K among the target systems, while the OU Ser system with 16 K had the lowest. Table 5 lists the temperature difference between companions. Based on the stars' effective temperatures, we estimated the spectral type of the stars using Cox [44] study (Table 5). We also checked the results of the effective temperature in this study

Table 4

ESTIMATED ABSOLUTE PARAMETERS OF 20 CONTACT BINARY SYSTEMS USING Gaia DR3 PARALLAX

System	$M_1(M_\odot)$	$M_2(M_\odot)$	$R_1(R_\odot)$	$R_2(R_\odot)$	$L_1(L_\odot)$	$L_2(L_\odot)$	M_{bol1}	M_{bol2}	$\log(g)_1$	$\log(g)_2$	$a(R_\odot)$
AC Boo	0.37(10)	1.23(35)	0.72(7)	1.23(11)	0.77(19)	1.87(46)	5.02(24)	4.05(24)	4.29(3)	4.35(4)	2.46(21)
AQ Psc	1.53(35)	0.39(14)	1.65(14)	0.91(8)	3.88(84)	0.96(21)	3.26(21)	4.78(22)	4.19(2)	4.11(6)	3.18(25)
BI CVn	0.49(11)	1.19(35)	0.88(9)	1.28(12)	1.02(26)	1.92(46)	4.71(25)	4.02(23)	4.24(1)	4.30(3)	2.64(22)
BX Dra	1.74(41)	0.45(11)	2.02(15)	1.15(9)	8.52(60)	2.91(55)	2.40(19)	3.57(19)	4.07(3)	3.97(3)	3.80(28)
BX Peg	0.37(11)	1.06(34)	0.62(6)	0.98(10)	0.39(11)	0.72(19)	5.75(26)	5.09(25)	4.43(3)	4.48(4)	2.03(19)
CC Com	0.43(14)	0.87(31)	0.55(6)	0.75(8)	0.10(3)	0.15(4)	7.22(29)	6.77(28)	4.59(3)	4.62(4)	1.68(18)
DY Cet	1.36(34)	0.47(13)	1.47(12)	0.93(8)	3.84(82)	1.44(31)	3.27(21)	4.33(21)	4.24(3)	4.17(4)	2.98(24)
EF Boo	0.62(15)	1.16(32)	0.99(9)	1.30(11)	1.50(33)	2.66(57)	4.29(22)	3.67(21)	4.23(2)	4.27(3)	2.86(23)
EX Leo	1.49(36)	0.26(11)	1.55(16)	0.73(10)	3.20(89)	0.73(25)	3.47(27)	5.07(32)	4.23(1)	4.12(5)	2.79(23)
FU Dra	0.30(9)	1.19(36)	0.61(6)	1.12(11)	0.46(11)	1.32(31)	5.58(23)	4.43(23)	4.35(3)	4.42(4)	2.19(20)
HV Aqr	1.42(39)	0.24(7)	1.45(13)	0.68(6)	3.37(73)	0.82(18)	3.41(21)	4.95(22)	4.27(3)	4.15(4)	2.59(22)
LO And	1.28(34)	0.39(12)	1.32(12)	0.79(8)	3.22(72)	1.08(27)	3.46(22)	4.65(24)	4.30(3)	4.23(4)	2.62(22)
OU Ser	1.28(34)	0.19(11)	1.21(16)	0.55(10)	1.55(51)	0.31(15)	4.25(31)	5.99(41)	4.38(1)	4.24(5)	2.13(20)
RW Com	0.87(24)	0.47(22)	0.78(11)	0.59(9)	0.29(10)	0.14(5)	6.08(33)	6.87(34)	4.59(1)	4.56(5)	1.78(18)
RW Dor	0.56(15)	0.88(30)	0.73(8)	0.89(10)	0.44(12)	0.57(16)	5.63(27)	5.33(27)	4.46(1)	4.48(4)	2.06(20)
RZ Com	0.47(13)	1.10(32)	0.78(7)	1.13(10)	0.90(22)	1.50(35)	4.84(23)	4.29(23)	4.32(3)	4.37(4)	2.37(21)
TW Cet	0.86(22)	0.66(23)	0.93(10)	0.82(9)	0.94(25)	0.65(18)	4.80(26)	5.20(26)	4.44(1)	4.42(4)	2.25(20)
UV Lyn	0.48(12)	1.28(35)	0.88(8)	1.36(12)	0.89(19)	1.87(40)	4.85(21)	4.05(21)	4.23(2)	4.28(3)	2.83(23)
UX Eri	1.22(27)	0.62(21)	1.36(14)	1.00(11)	2.48(67)	1.08(31)	3.74(26)	4.65(27)	4.26(1)	4.23(4)	3.01(24)
VW Boo	0.47(12)	1.11(34)	0.76(7)	1.12(11)	0.47(12)	0.87(21)	5.54(25)	4.89(24)	4.35(2)	4.39(4)	2.40(21)

with the reports of Gaia and TESS, so that the difference is less than 5%.

Additionally, EX Leo, HV Aqr, and OU Ser are low mass ratio contact systems with values of 0.172(28), 0.168(23), and 0.149(24), respectively. Although these three systems have a low mass ratio, they are not close to the extremely low mass ratio cutoff, which is less than 0.1 [45]. On the other hand, we have three systems (BX Dra, HV Aqr, OU Ser) with fillout factors greater than 50% and mass ratios less than 0.25. These specifications relate to deep overcontact binaries suggested by the Qian et al. [46] study, which found that this type of star is likely to be the progenitor of a blue straggler/FK Com-type star [47,45].

We estimated the absolute parameters using the semi-major axis and orbital period relationship. So, some values from the light curve solutions ($T_{1,2}$, q, $r_{mean1,2}$), and the orbital period used in the calculation process.

The positions of the stars were displayed using the Zero-Age Main Sequence (ZAMS) and the Terminal-Age Main Sequence (TAMS) on the Mass-Luminosity (M - L) and Mass-Radius (M - R) diagrams, based on the absolute parameters (Fig.3a, b). Additionally, the outcomes have been compared with the theoretical fits from the study Poro et al. [10], and as expected the M - L and M - R

Table 5

THE SPECTRAL TYPE (Sp) OF STARS, TEMPERATURE DIFFERENCE OF COMPANIONS, TOTAL MASS, ORBITAL ANGULAR MOMENTUM, AND SUBTYPE OF THE TARGET BINARY SYSTEMS

System	Sp Star1	Sp Star2	ΔT (K)	$M_{tot}\,(M_{\odot})$	J_0	Subtype
AC Boo	F5	F8	287	1.60(46)	51.53(18)	W
AQ Psc	F6	G1	330	1.92(49)	51.67(19)	A
BI CVn	F8	G0	176	1.68(46)	51.65(17)	W
BX Dra	F1	F1	72	2.19(52)	51.80(16)	W
BX Peg	G3	K0	465	1.43(45)	51.45(20)	W
CC Com	K5	K5	215	1.30(46)	51.41(21)	W
DY Cet	F3	F3	97	1.83(48)	51.69(17)	A
EF Boo	F5	F5	40	1.77(47)	51.74(17)	A
EX Leo	F7	F7	45	1.74(47)	51.46(21)	W
FU Dra	G0	G3	242	1.49(45)	51.42(19)	W
HV Aqr	F5	F3	154	1.66(46)	51.41(18)	W
LO And	F2	F3	94	1.67(46)	51.58(18)	A
OU Ser	G3	G3	16	1.47(45)	51.25(26)	A
RW Com	K3	K3	193	1.33(45)	51.45(23)	A
RW Dor	G8	K0	188	1.44(45)	51.55(19)	W
RZ Com	F5	G0	355	1.57(45)	51.58(18)	W
TW Cet	G2	G6	191	1.51(45)	51.62(19)	A
UV Lyn	G0	G3	201	1.76(47)	51.67(17)	W
UX Eri	F7	G2	336	1.84(48)	51.77(18)	A
VW Boo	G8	K0	237	1.58(46)	51.59(18)	W

connections are weak. Fig.3c shows the position of the systems compared to the q - L_{ratio} theoretical fit obtained from the study Poro et al. [10], with which they are in good agreement. We utilized the following equation from the study Eker et al. [48] to calculate the orbital angular momentum J_0 of the systems:

$$J_0 = \frac{q}{(1+q)^2}\sqrt[3]{\frac{G^2}{2\pi}M^5 P}\,, \tag{7}$$

where q is the mass ratio, M is the total mass of the system, P is the orbital period, and G is the gravitational constant. The results of estimating the J_0 are listed in Table 5 along with the total mass of the systems. We also determined the subtype of each system (Table 5). Therefore, we considered the systems where the more massive star has a hotter effective temperature than the companion as A-type and otherwise as W-type. Additionally, the target systems' position is depicted in the $\log M_{tot}$ - $\log J_0$ diagram (Fig.3d), which indicates that they are in a contact binary systems region.

The temperature-mass relationship for contact binary systems was presented

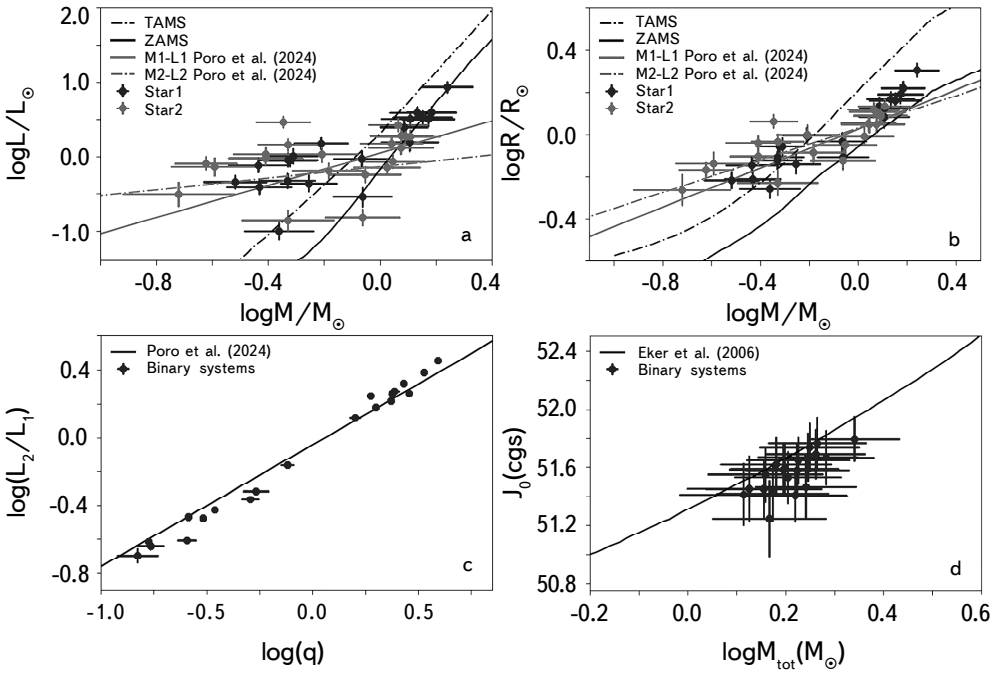

Fig.3. (a) $M_{1,2}$ - $L_{1,2}$, (b) $M_{1,2}$ - $R_{1,2}$, (c) q - L_{ratio}, and (d) M_{tot} - J_0 diagrams.

by Poro et al. [49] with a linear fit. They made use of 428 contact systems from the study [6] sample. The hotter component T_h and the mass of the more massive star M_m were considered for this relation by Poro et al. [49]. Our target systems are positioned on the T_h - M_m diagram (Fig.4), which indicates good agreement with the theoretical fit and uncertainty.

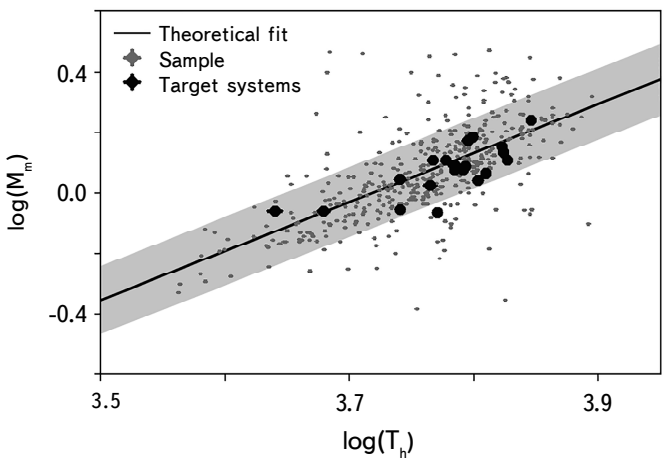

Fig.4. The diagram of the relationship between the effective temperature T_h and the mass M_m of the primary component in contact binary stars in which the studied systems are displayed.

Acknowledgements. This manuscript was prepared by the BSN project (https://bsnp.info/). We used data from the European Space Agency's mission Gaia (http://www.cosmos.esa.int/gaia). We made use of the SIMBAD database, which is operated by CDS in Strasbourg, France (http://simbad.u-strasbg.fr/simbad/). This work includes data from the TESS mission observations. Funding for the TESS mission is provided by the NASA Explorer Program. We acknowledge the TESS team for its support of this study.

Binary Systems of South and North (BSN) Project, Tehran, Iran, e-mail: atilaporo@bsnp.info

АНАЛИЗ КРИВЫХ БЛЕСКА И АБСОЛЮТНЫХ ПАРАМЕТРОВ ДВАДЦАТИ КОНТАКТНЫХ ДВОЙНЫХ ЗВЕЗД С ИСПОЛЬЗОВАНИЕМ ДАННЫХ TESS

Э.ПАКИ, А.ПОРО

Анализ контактных двойных звезд с использованием фотометрических данных космических телескопов и исследование возможных изменений параметров могут дать точную картину для теоретических исследований. Мы исследовали решения световых кривых и фундаментальные параметры для двадцати контактных двойных систем. Для анализа использовались самые последние данные спутника для исследования транзитных экзопланет (TESS). Исследованные в данной работе системы имеют орбитальный период менее 0.58 дня. Решения световых кривых были получены с использованием Python-кода PHOEBE версии 2.4.9. Результаты показывают, что системы имели различные соотношения масс от $q=0.149$ до $q=3.915$, коэффициенты заполнения (степень контакта) от $f=0.072$ до $f=0.566$ и наклоны от $i=52^{\circ}.8$ до $i=87^{\circ}.3$. Эффективная температура звезд была менее 7016 K, как и ожидалось, учитывая особенности большинства контактных двойных звезд. Кривые блеска двенадцати из целевых систем были асимметричны в максимумах, показывая эффект О'Коннелла, и для решений световых кривых требовалось наличие звездного пятна. Были представлены и обсуждены оценки абсолютных параметров двойных систем с использованием эмпирической зависимости a - P. Рассчитаны орбитальные угловые моменты J_0 систем. Положения систем представлены на диаграммах M - L, M - R, q - L_{ratio}, M_{tot} - J_0 и T - M.

Ключевые слова: *двойная звезда: затмение - двойные звезды: близкие - анализ данных*

REFERENCES

1. *Z.Kopal*, Close binary systems. The International Astrophysics Series, London: Chapman & Hall, 1959.
2. *G.P.Kuiper*, Astrophys. J., **93**, 133, 1941.
3. *K.Yakut*, *P.P.Eggleton*, Astrophys. J., **629**, 1055, 2005. doi:10.1086/431300.
4. *L.Binnendijk*, Vistas in Astronomy, **12**, 217, 1970.
5. *L.B.Lucy*, *R.E.Wilson*, Astrophys. J., **231**, 502, 1979. doi:10.1086/157212.
6. *O.Latković*, *A.Čeki*, *S.Lazarević*, Astrophys. J. Suppl., **254**, 10, 2021. doi:10.3847/1538-4365/abeb23.
7. *G.A.Loukaidou*, *K.D.Gazeas*, *S.Palafouta et al.*, Mon. Not. Roy. Astron. Soc., **514**, 5528, 2022. doi:10.1093/mnras/stab3424.
8. *X.-D.Zhang*, *S.-B.Qian*, Mon. Not. Roy. Astron. Soc., **497**, 3493, 2020. doi:10.1093/mnras/staa2166.
9. *D.J.K.O'Connell*, PRCO, **2**, 85, 1951.
10. *A.Poro*, *E.Paki*, *A.Alizadehsabegh et al.*, RAA, **24**, 015002, 2024. doi:10.1088/1674-4527/ad0866.
11. *K.Li*, *Q.-Q.Xia*, *C.-H.Kim et al.*, Astron. J., **162**, 13, 2021. doi:10.3847/1538-3881/abfc53.
12. *M.F.Yıldırım*, 2022, RAA, 22, 055013. doi:10.1088/1674-4527/ac5ee8.
13. *G.R.Ricker*, *D.W.Latham*, *R.K.Vanderspek et al.*, AAS, 2010.
14. *K.G.Stassun*, *R.J.Oelkers*, *J.Pepper et al.*, Astron. J., **156**, 102, 2018. doi:10.3847/1538-3881/aad050.
15. *E.F.Schlafly*, *D.P.Finkbeiner*, Astrophys. J., **737**, 103, 2011. doi:10.1088/0004-637X/737/2/103.
16. *G.M.Green*, *E.Schlafly*, *C.Zucker et al.*, Astrophys. J., **887**, 93, 2019. doi:10.3847/1538-4357/ab5362.
17. *A.Prša*, *K.E.Conroy*, *M.Horvat et al.*, Astrophys. J. Suppl., **227**, 29, 2016. doi:10.3847/1538-4365/227/2/29.
18. *S.M.Ruciński*, AcA, **19**, 245, 1969.
19. *L.B.Lucy*, ZA, **65**, 89, 1967.
20. *F.Castelli*, *R.L.Kurucz*, arXiv preprint astro-ph/0405087.
21. *K.Sriram*, *S.Malu*, *C.S.Choi*, Astron. J., **153**, 231, 2017. doi:10.3847/1538-3881/aa6893.
22. *R.H.Nelson*, IBVS, **5951**, 1, 2010.
23. *S.Deb*, *H.P.Singh*, Mon. Not. Roy. Astron. Soc., **412**, 1787, 2011. doi:10.1111/j.1365-2966.2010.18016.x.
24. *R.H.Nelson*, *H.V.Şenavci*, *Ö.BaŞtürk et al.*, NewA, **29**, 57, 2014. doi:10.1016/j.newast.2013.11.006.
25. *J.-H.Park*, *J.W.Lee*, *S.-L.Kim et al.*, PASJ, **65**, 1, 2013. doi:10.1093/pasj/65.1.1.
26. *K.Li*, *S.Hu*, *D.Guo et al.*, NewA, **41**, 17, 2015. doi:10.1016/j.newast.2015.04.010.
27. *O.Köse*, *B.Kalomeni*, *V.Keskin et al.*, Astron. Nachr., **332**, 626, 2011. doi:10.1002/

asna.201011566.
28. *K.D.Gazeas*, *A.Baran*, *P.Niarchos et al.*, AcA, **55**, 123, 2005.
29. *S.Zola*, *K.Gazeas*, *J.M.Kreiner et al.*, Mon. Not. Roy. Astron. Soc., **408**, 464, 2010. doi:10.1111/j.1365-2966.2010.17129.x.
30. *L.Liu*, *S.-B.Qian*, *J.-J.He et al.*, PASJ, **64**, 48, 2012. doi:10.1093/pasj/64.3.48.
31. *K.Li*, *S.-B.Qian*, NewA, **21**, 46, 2013. doi:10.1016/j.newast.2012.11.003.
32. *R.H.Nelson*, *R.M.Robb*, IBVS, **6134**, 1, 2015.
33. *T.Sarotsakulchai*, *S.-B.Qian*, *B.Soonthornthum et al.*, PASJ, **71**, 34, 2019. doi:10.1093/pasj/psy149.
34. *R.H.Nelson*, *K.B.Alton*, IBVS, **6266**, 1, 2019. doi:10.22444/IBVS.6266.
35. *S.Zola*, *J.M.Kreiner*, *B.Zakrzewski et al.*, AcA, **55**, 389, 2005.
36. *L.Liu*, *S.-B.Qian*, *L.-Y.Zhu et al.*, Astron. J., **141**, 147, 2011. doi:10.1088/0004-6256/141/5/147.
37. *F.Tavakkoli*, *A.Hasanzadeh*, *A.Poro*, New Astron., **37**, 64, 2015. doi:10.1016/j.newast.2014.12.004.
38. *A.Poro*, *E.Fernández-Lajús*, *M.Madani et al.*, RAA, **23**, 095011, 2023. doi:10.1088/1674-4527/ace027.
39. *A.Poro*, *M.Tanriver*, *R.Michel et al.*, Publ. Astron. Soc. Pacif., **136**, 024201, 2024. doi:10.1088/1538-3873/ad1ed3.
40. *A.Poro*, *M.Hedayatjoo*, *M.Nastaran et al.*, New Astron., **110**, 102227, 2024. doi:10.1016/j.newast.2024.102227.
41. *A.Poro*, *S.Zamanpour*, *M.Hashemi et al.*, New Astron., **86**, 101571, 2021. doi:10.1016/j.newast.2021.101571.
42. *S.Kouzuma*, Astrophys. J., **958**, 84, 2023. doi:10.3847/1538-4357/ad03e1.
43. *G.Torres*, Astron. J., **140**, 1158, 2010. doi:10.1088/0004-6256/140/5/1158.
44. *A.N.Cox*, Allen's Astrophysical Quantities, AlP Press, Springer, New York, 2000.
45. *K.Li*, *Q.-Q.Xia*, *C.-H.Kim et al.*, Astrophys. J., **922**, 122, 2021. doi:10.3847/1538-4357/ac242f.
46. *S.-B.Qian*, *Y.-G.Yang*, *B.Soonthornthum et al.*, Astron. J., **130**, 224, 2005. doi:10.1086/430673.
47. *Y.-G.Yang*, *S.-B.Qian*, *L.-Y.Zhu et al.*, Astron. J., **138**, 540, 2009. doi:10.1088/0004-6256/138/2/540.
48. *Z.Eker*, O.Demircan, *S.Bilir et al.*, Mon. Not. Roy. Astron. Soc., **373**, 1483, 2006. doi:10.1111/j.1365-2966.2006.11073.x.
49. *A.Poro*, *S.Baudart*, *M.Nourmohammad et al.*, RAA, **24**, 055001, 2024. doi:10.1088/1674-4527/ad3a2c.